Research Article

GAZİ
JOURNAL OF ENGINEERING SCIENCES

Optimization of Tensile Properties in 3D-Printed PETG Honeycomb Structures via Taguchi Method: Influence of Cell Size and Geometric Orientation

Ahmet Fatih Yılmaz*[a]

Submitted: 04.03.2025 Revised: 24.04.2025 Accepted: 28.04.2025 doi:10.30855/gmbd.070525N11

ABSTRACT

Honeycomb structures are extensively used in engineering applications due to their high strength-to-weight ratio, energy absorption capacity, and customizable mechanical behavior. However, optimizing their tensile performance remains a significant challenge. This study systematically investigates the effects of cell size (1.75 mm, 1.5 mm, 1.25 mm) and geometric orientation (0°, 15°, 30°) on the tensile behavior of 3D-printed PETG honeycomb structures, fabricated using FDM. Nine different specimens were manufactured and tested following the ASTM D638 standard. The optimal configuration was determined using Taguchi's signal-to-noise (S/N) ratio analysis, while Analysis of Variance (ANOVA) was conducted for statistical evaluation. The results indicate that a cell size of 1.25 mm and a 30° orientation provided the highest fracture force (277.03 N), while the 1,75 mm cell size at 30° exhibited the greatest energy absorption (335.59×10^{-3} J). ANOVA confirmed that cell size significantly influenced tensile strength, whereas geometric orientation had a greater impact on energy absorption. This study contributes to optimizing three-dimensional (3D) printing parameters for enhanced mechanical performance and provides insights for designing lightweight, high-strength structures in aerospace and structural applications.

Keywords: Honeycomb structures, FDM, Taguchi optimization, PETG, Mechanical properties

[a,*] Karabuk University,
Engineering Faculty,
Dept. of Mechanical Engineering
78100-Karabük, Türkiye
Orcid: 0000-0001-5784-0121
e mail: ahmetfatihyilmaz@karabuk.edu.tr

*Corresponding author:
ahmetfatihyilmaz@karabuk.edu.tr

Taguchi Yöntemi ile 3B Baskılı PETG Bal Peteği Yapılarında Çekme Özelliklerinin Optimizasyonu: Hücre Boyutu ve Geometrik Yönelimin Etkisi

ÖZ

Bal peteği yapıları, yüksek mukavemet/ağırlık oranı, enerji sönümleme kapasitesi ve özelleştirilebilir mekanik davranışları nedeniyle mühendislik uygulamalarında yaygın olarak kullanılmaktadır. Ancak, çekme dayanımının optimize edilmesi halen önemli bir araştırma konusudur. Bu çalışma, hücre boyutu (1.75 mm, 1.5 mm, 1.25 mm) ve geometrik yönelim (0°, 15°, 30°) değişkenlerinin, EYM yöntemiyle üretilen PETG bal peteği yapılarının çekme mekanik özellikleri üzerindeki etkisini sistematik olarak incelemektedir. Toplamda dokuz farklı numune üretilmiş ve ASTM D638 standardına uygun olarak test edilmiştir. Taguchi sinyal-gürültü (S/N) oranı analizi ile optimum parametreler belirlenmiş, Varyans Analizi (ANOVA) ile istatistiksel değerlendirme yapılmıştır. Sonuçlar, 1.25 mm hücre boyutu ve 30° yönelime sahip yapıların en yüksek kırılma kuvvetine (277.03 N) ulaştığını, 1.75 mm hücre boyutu ve 30° yönelimdeki numunelerin ise en yüksek enerji sönümleme kapasitesine (335.59×10^{-3} J) sahip olduğunu göstermektedir. ANOVA analizleri, hücre boyutunun çekme dayanımı üzerinde önemli bir etkiye sahip olduğunu, geometrik yönelimin ise enerji sönümleme kapasitesini daha fazla etkilediğini doğrulamıştır. Bu çalışma, üç boyutlu (3D) baskı parametrelerinin mekanik performans açısından optimize edilmesine katkı sağlamakta ve havacılık ile yapısal uygulamalar için hafif ve yüksek dayanımlı yapıların tasarımına yönelik önemli bilgiler sunmaktadır.

Anahtar Kelimeler: Bal peteği yapıları, EYM, Taguchi yöntemi, PETG, Mekanik özellikler

To cite this article: A. F. Yilmaz, "Optimization of Tensile Properties in 3D-Printed PETG Honeycomb Structures via Taguchi Method: Influence of Cell Size and Geometric Orientation", *Gazi Journal of Engineering Sciences*, vol.11, no.1, pp. 167-178, 2025. doi:10.30855/gmbd.070525N11

1. Introduction

The growing need for lightweight to high strength materials in aerospace, automotive, biomedical, and structural applications has driven significant interest in honeycomb structures. These structures provide exceptional mechanical properties such as a high strength to weight ratio, superior energy absorption, and customizable deformation behavior [1]. Advances in additive manufacturing (AM), especially Fused Deposition Modeling (FDM), have enabled the precise fabrication of intricate honeycomb geometries using various thermoplastic materials [2]. Among these, polyethylene terephthalate glycol-modified (PETG) is a popular choice due to its excellent balance of mechanical performance, durability, and printability [3]. However, the performance of 3D-printed honeycomb structures is highly dependent on cell size, geometric orientation, and printing parameters, which remain an open field of optimization. Optimizing these parameters is crucial for ensuring reliable mechanical performance while minimizing material waste and production time. By employing the Taguchi optimization method, this research seeks to systematically explore the influence of cell size and geometric orientation on the tensile behavior of PETG honeycomb structures, thereby providing valuable insights for performance-driven design improvements [4].

A honeycomb structure consists of a periodic arrangement of hollow cells, typically hexagonal, rectangular, or auxetic in shape, designed to optimize mechanical properties while minimizing material usage [5]. Fused Deposition Modeling (FDM) is an additive manufacturing technique that extrudes thermoplastic filaments layer-by-layer to create 3D-printed objects. PETG is a widely used polymer in FDM printing due to its high impact resistance, ductility, and chemical resistance compared to other common materials such as PLA and ABS [6]. The Taguchi optimization method is a statistical approach used to determine the most influential parameters affecting product performance while reducing experimental iterations [7].

Numerous studies have investigated the mechanical behavior of honeycomb structures manufactured using 3D printing. Recent advancements focus on understanding how geometric variations, printing orientation, and cell design affect mechanical properties, since gaps remain in systematically optimizing these parameters for tensile performance [8]. Several research efforts have explored the effects of honeycomb geometry and printing parameters. Studies have found that hexagonal honeycombs offer superior mechanical properties compared to square or triangular designs due to their higher in-plane stiffness and energy absorption capacity [9]. Other studies indicate that the orientation of printed layers significantly impacts mechanical strength, with vertical and diagonal orientations often displaying lower strength due to weak interlayer adhesion [10]. PETG has gained attention as a favorable material due to its higher ductility and impact resistance compared to PLA and ABS, making it appropriate for high performance applications [11]. The use of optimization methodologies, including statistical and computational approaches, has shown potential in improving honeycomb structure performance [12]. Taguchi and response surface methodologies have been applied in optimizing 3D-printing parameters, particularly for impact and compressive strength [13]. Moreover, several computational and experimental studies have examined the mechanical performance of honeycomb structures. Finite Element Analysis (FEA) models have been developed to predict compressive and bending behavior of different honeycomb cell configurations [14]. Experimental studies have explored the anisotropic mechanical properties of FDM-printed structures with varying infill densities and orientations [15]. FFT-based modeling techniques have also been proposed to enhance the predictive accuracy of in plane elastic properties of honeycomb structures beneath large elastic deformations [16]. Recent advancements in integrating machine learning and AI-based models have enhanced mechanical prediction accuracy of honeycomb structures [12]. However, while these studies provide valuable insights, the impact of cell size and geometric orientation on tensile properties remains underexplored. Moreover, a few studies have employed robust optimization techniques such as Taguchi methods to fine-tune design parameters for optimal tensile strength [17]. Despite the extensive research on honeycomb structures and their mechanical properties, several gaps and limitations persist. Most studies focus on compressive or bending performance, neglecting tensile properties, which are critical in structural applications [18]. There has been limited investigation on the combined effects of cell size and geometric orientation in PETG honeycombs [19]. Few studies have

employed systematic optimization using the Taguchi method for enhancing tensile performance. Challenges remain in accurately modeling the anisotropic behavior of FDM-printed structures due to interlayer adhesion issues and print-induced defects [20]. In addition, the thermo-mechanical interactions in honeycomb materials require further modeling efforts [21]. Recent studies have explored bioinspired functionally graded honeycomb structures, revealing promising impact resistance properties [22]. Moreover, efforts to enhance energy absorption capabilities in honeycomb structures are ongoing, especially for corrugated honeycomb aluminum designs [23]. These limitations highlight the need for an optimized approach to improve the tensile behavior of PETG honeycomb structures, guiding the development of lightweight to high-strength materials.

This research aims to examine the effect of honeycomb cell size and geometric orientation on the tensile properties of 3D-printed PETG structures. The research employs the Taguchi optimization method to determine the most influential parameters for maximizing tensile strength. Furthermore, the study provides experimental validation and statistical analysis to guide optimal design configurations for PETG honeycomb-based applications. This investigation is particularly significant for its originality, as it is among few to investigate the impact and optimization of geometric orientation and cell size on the tensile mechanical properties of FDM-printed PETG honeycomb structures. Consequently, 9 distinct specimens were fabricated utilizing 3 different cell sizes (1,25 mm, 1,5 mm, 1.75 mm) and 3 different geometric orientations (0°, 15°, and 30°) through the FDM technique using the same PETG material. The Taguchi method was utilized to optimize the maximum fracture force and energy absorption by determining the optimum combination of cell size and geometric orientation. The results were additionally examined utilizing analysis of variance (ANOVA). This study aimed to address a gap in literature by investigating the tensile properties of honeycomb structures printed using FDM-printed PETG.

2. Material And Method

2.1. Design of honeycomb structure

The ASTM D638-14 standards employed a dog-bone-shaped specimen with appropriately placed honeycomb structures within the testing section for the tension test [24]. Specimen dimensions were obtained from a Type IV model, as shown in Figure 1, and SolidWorks software was chosen to create the computer-aided design (CAD) shape.

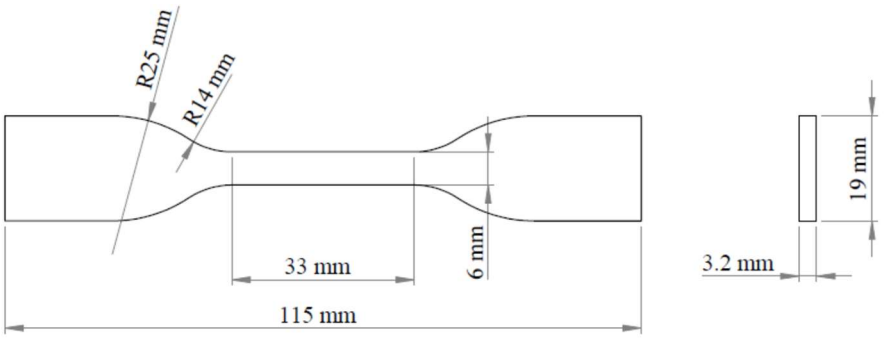

Figure 1. The geometry of the experimental specimen, based on ASTM D638-14 standards.

The tensile test specimens had a thickness of 0.6 mm (2h and were designed to accommodate 2, 3, and 4 honeycomb unit cells, as illustrated in Figure 2, within the 6 mm width of the test zone in the 0° geometric orientation. Consequently, cell sizes (c) of 1.75 mm, 1.5 mm, and 1.25 mm were selected based on minimum and maximum value constraints, considering both design objectives and manufacturability. Additionally, geometric orientation values of 0°, 15°, and 30° were chosen within the specified range of minimum, maximum, and average values.

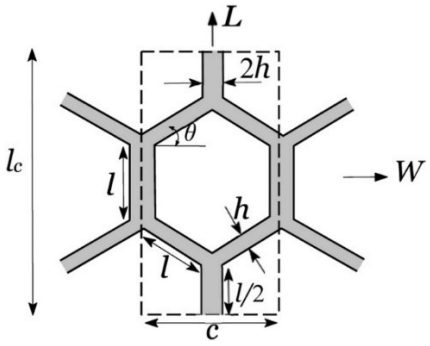

Figure 1. The unit cell of the honeycomb structure.

These cells were then rotated by 15° and 30° and placed in the test area and then the geometric orientations of the honeycomb structures were designed using SolidWorks software as shown in Figure 3, resulting in three distinct plans (0°, 15°, 30°).

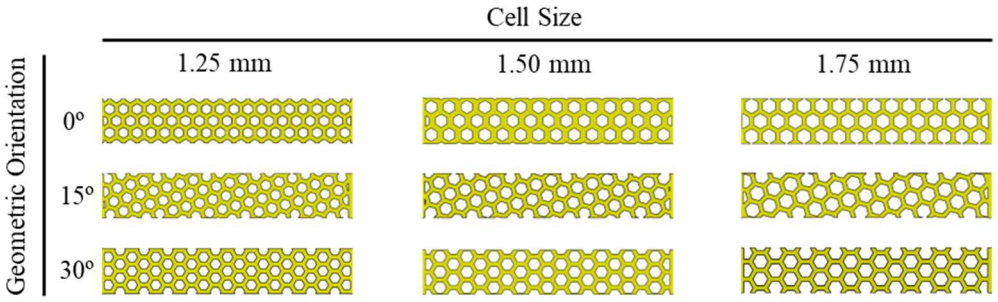

Figure 2. Designs of the test areas of the tensile specimens.

2.2. Manufacturing test specimens

The honeycomb structures were first saved as STL files and then imported into the Ultimaker Cura slicing software to define the print settings and optimize the arranging of the specimens on the build plate. The specimens were fabricated using polyethylene terephthalate glycol (PETG) filament with a Creality Ender 3 Pro 3D printer. The study followed the recommended print settings for PETG, specifically a layer height of 0.2 mm, a speed of print is 50 mm/s, a lines infill pattern, and an infill density of 25%. Figure 4 presents images of the fabricated specimens in the test area.

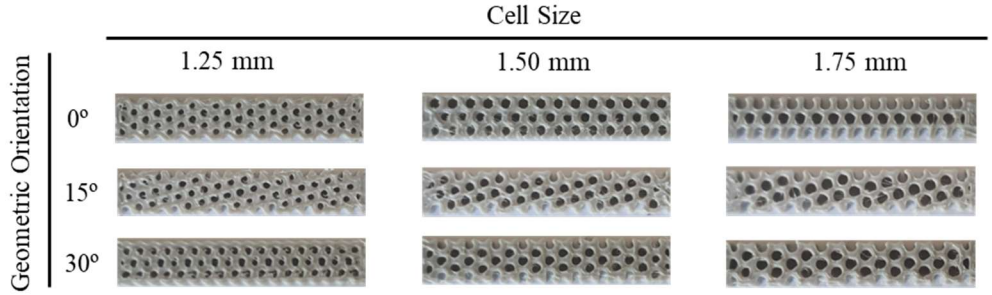

Figure 3. Images of the test areas of the manufactured tensile specimens.

In accordance with the principles of Design of Experiments (DOE) methodology, a total of nine distinct specimens were manufactured, as shown in Figure 5. To minimize the influence of random error sources and variability, three specimens were produced for each sample.

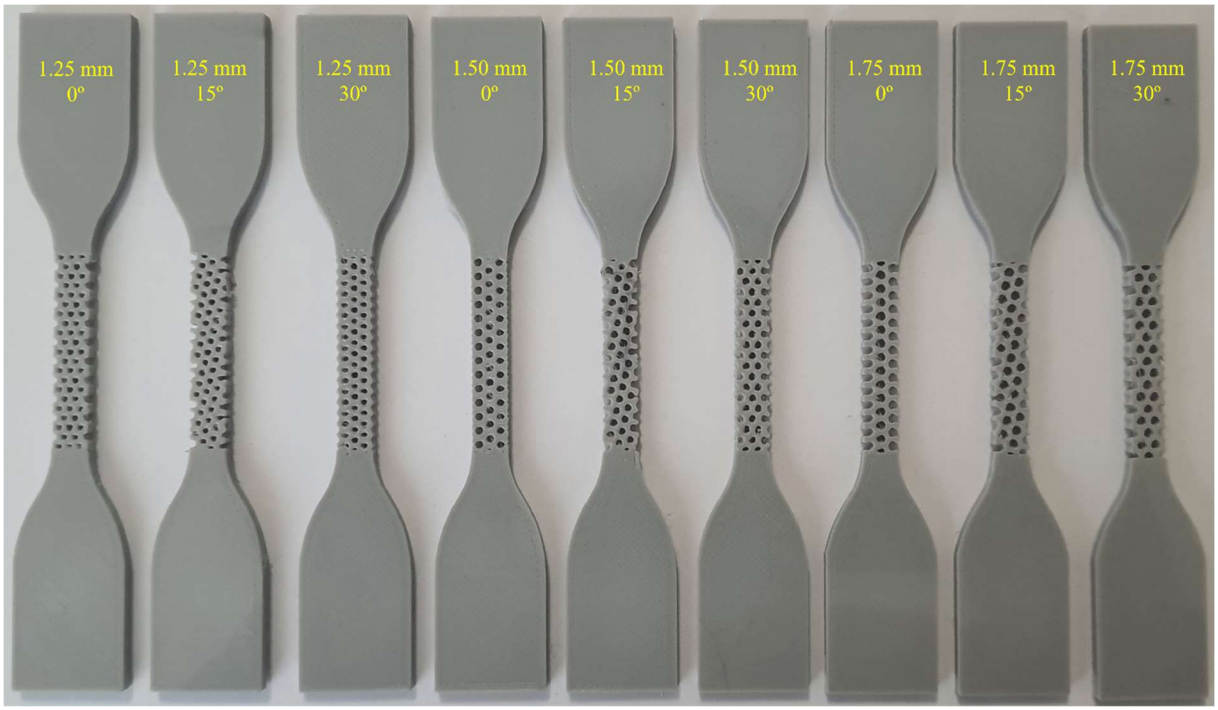

Figure 4. 3d printed tensile specimens.

2.3. Tensile Test

The tensile test was accomplished utilizing a Shimadzu Autograph universal testing machine in compliance with the ASTM D638 standard. The displacement rate was adjusted at 5 mm/min, and the specimens were subjected to a gradually increasing load until failure. Load and displacement data were systematically recorded during the experiment and subsequently analyzed to determine the mechanical properties. A representative tensile test specimen is shown in Figure 6.

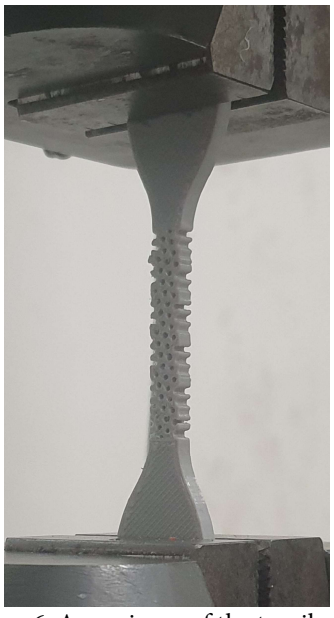

Figure 6. A specimen of the tensile test.

2.3. Optimization

The Taguchi method offers a statistically robust approach that facilitates the identification of optimal operating conditions while reducing the number of required experiments, thus reducing both the time and cost associated with experimental investigations [25]. A major advantage of this method is its use of orthogonal arrays for experimental design, which not only simplifies the planning process but also accounts for uncontrolled variables commonly referred to as noise factors that contribute to variability.

In this study, a full factorial design was employed, incorporating two factors at three levels each, to systematically explore their interactions and effects on a specified response variable [26]. The primary factors influencing force at break and energy absorption were identified as the dimensions and orientations of the honeycomb structures. Table 1 presents these factors alongside their respective levels.

Table 1. Taguchi L9 orthogonal array.

Factors		**Levels**	
Cell size	1.75 mm	1.5 mm	1.25 mm
Geometric orientation	0°	15°	30°

To optimize the experimental design, Taguchi's L9 orthogonal array was chosen. The experimental setup was designed using Minitab's L9 Taguchi orthogonal array, facilitating the generation of main effects plots for the signal-to-noise (S/N) ratio related to mechanical properties. Given that the primary objective of this study was to enhance tensile strength specifically, force at break and energy absorption the "larger-is-better" criterion was applied in accordance with Equation (1).

$$S/N = -10\log_{10}\left[\frac{1}{n}\sum_{i=1}^{n}\frac{1}{y_i{}^2}\right] \quad (1)$$

3. Results and Discussion

This section analyzes the mechanical performance of three individual honeycomb structures with varying geometric orientations, as determined through tensile testing. The tensile tests were conducted to evaluate the force at break and absorbed energy, with each measurement averaged across multiple specimens. The mean values, along with their standard deviations, are presented in Table 2. The results indicate that the highest force at break was recorded at 277.03 N in run 9, whereas the lowest value was observed in run 1 at 128.43 N. Similarly, absorbed energy varied across the samples, with run 3 exhibiting the highest value of 335.59×10^{-3} J and run 5 the lowest at 151.95×10^{-3} J. Based on these findings, the optimal combination of cell size and geometric orientation for maximizing both force at break and absorbed energy is 1.25 mm and 30°, respectively, yielding values of 277.03×10^{-3} J and 288.47×10^{-3} J. In order to further improve the clarity and interpretability of the results, descriptive statistical data are presented in Table 2. These data include the minimum and maximum values, mean values, and standard deviations for each test run.

Table 2. Results of the tensile test.

Run	Cell size	Geometric orientation	Force (N)	Energy (x10-3 J)
1	1.75 mm	0°	128.43	165.64
2	1.75 mm	15°	137.10	200.69
3	1.75 mm	30°	164.06	335.59
4	1.50 mm	0°	143.75	272.74
5	1.50 mm	15°	141.66	151.95
6	1.50 mm	30°	146.87	130.26
7	1.25 mm	0°	253.62	220.26
8	1.25 mm	15°	169.732	152.74
9	1.25 mm	30°	277.03	288.47

Figure 7 illustrates the force-displacement curves obtained from tensile tests conducted on specimens with honeycomb cell orientations of 0°, 15°, and 30°, across three different cell sizes within the test area: 1.75 mm, 1.5 mm, and 1.25 mm. For the 1.75 mm cell size configuration, the 30° orientation exhibited the highest force resistance, whereas the 0° and 15° orientations demonstrated lower force responses. Notably, the 15° orientation experienced structural failure at an elongation of approximately 1.68 mm. In the 1.50 mm cell size configuration, the 30° orientation continued to show the highest force at break. The 0° and 15° orientations followed trends similar to those observed in the 1.75 mm configuration, displaying a gradual increase in force until failure; however, in this case, their force values were closer to the 30° orientation. The overall force capacity in this configuration exceeded that of the 1.75 mm cell size, indicating that increasing the number of cells enhances the structural strength of the specimen. The 1.25 mm cell size configuration maintained this trend, with the 30° orientation again exhibiting the highest force resistance, reaching a peak force of approximately 290 N. This suggests that reducing the cell size results in a structure with greater strength and stiffness. The 0° and 15° orientations demonstrated comparable behavior, though they exhibited slightly higher force values prior to yielding compared to the larger cell size configurations.

Figure 8 illustrates the force-displacement curves obtained from tensile tests performed on specimens with varying geometric orientations of 0°, 15°, and 30°. Each graph presents a comparative analysis of three different cell size configurations: 1.75 mm, 1.50 mm, and 1.25 mm. In the 0° geometric orientation, the specimen with a 1.25 mm cell size exhibits the highest force capacity, followed by the 1.50 mm and 1.75 mm configurations, which display similar values. This observation aligns with findings in the existing literature, which suggest that specimens with smaller cell sizes can endure greater forces before structural failure [23]. The force-displacement curve for the 1.25 mm configuration shows a significant increase in force, indicative of a stronger material response, whereas the 1.75 mm configuration exhibits a comparatively lower force resistance. For the 15° geometric orientation, the force capacities of all three cell sizes are closely aligned, in contrast to the more pronounced differences observed in the 0° and 30° orientations. This behavior is unique and noteworthy from a structural perspective. Nonetheless, the 1.25 mm cell size configuration continues to demonstrate the highest force resistance. While the displacement at failure remains consistent across configurations, it is slightly lower than that observed in the 0° orientation. In the 30° geometric orientation, the specimen with a 1.25 mm cell size once again exhibits the highest force capacity, followed closely by the 1.75 mm configuration. In contrast, the 1.50 mm cell size displays the lowest force resistance, showing a significant difference compared to the other configurations. The displacement patterns in this orientation resemble those observed in the 0° configuration. This suggests that the material maintains its structural integrity in the 30° orientation almost as effectively as in the 0° orientation.

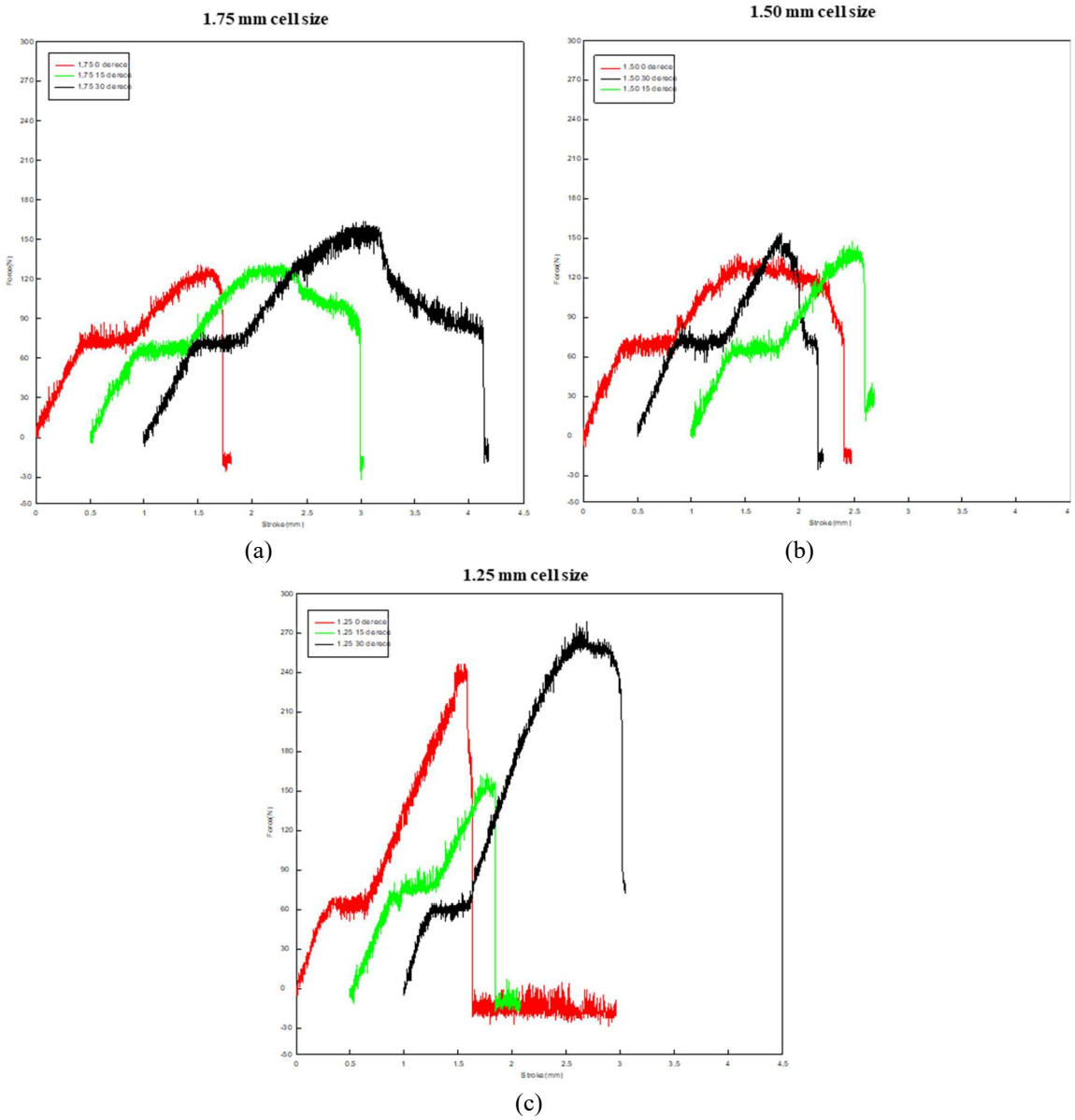

Figure 5. Force-displacement curves of tensile specimens containing different cell sizes in the test area (a) 1.75 mm, (b) 1.50 mm and (c) 1.25 mm.

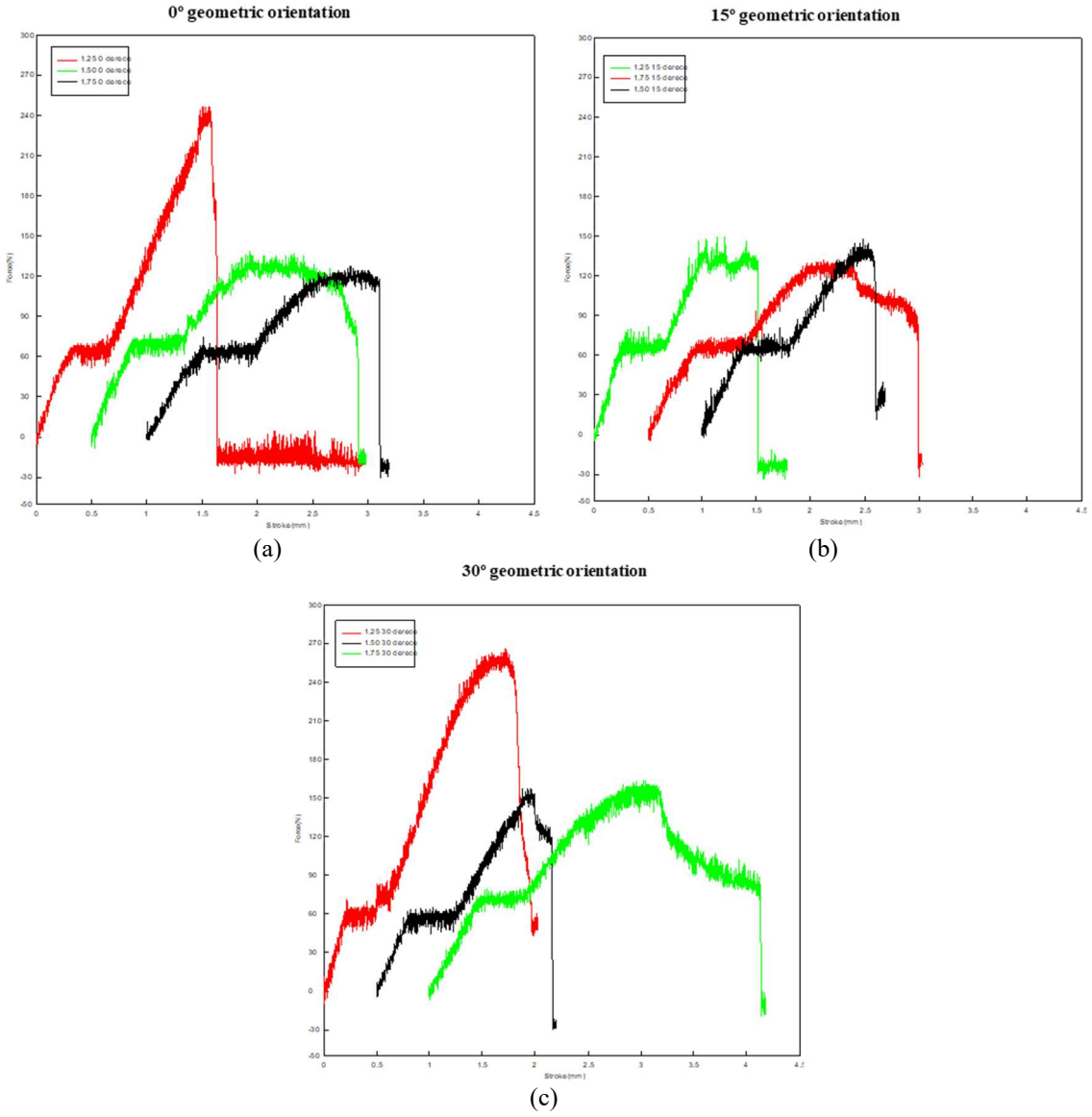

Figure 6. Force-displacement curves of tensile specimens containing different geometric orientations in the test area (a) 0°, (b) 15° and (c) 30°.

Table 3 shows that the influence of cell size and geometric orientation of the honeycomb structure on force at break and absorbed energy. As seen in the table, while cell size is 69.53% on force at break, it's only 9.38% on absorbed energy. And also, for geometric orientation, there is reverse contribution on force at break and absorbed energy. Geometric orientation effect is 14.03% whereas it is significantly higher than in absorbed energy as 25.68%. Most models with P-values above 0.05 are worthless, but a component with a P-value below 0.05 definitely influenced the final model [27,28]. The P-values are below 0.05 only on the effect of cell size on force at break within four values as indicated in Table 3. The cell size of the honeycomb structure has a P value higher than 0.05 for absorbed energy. However geometric orientation of the honeycomb structure has a P-value higher than 0.05 both on force at break and absorbed energy. As with different porous structures [29], for honeycomb structure, cell size is an important determinant for the force at break. Additionally, a computational technique for model validation has made use of the coefficient of determination R2. A strong correlation between experimental results and model predictions is indicated by R2 values near to 1 [30]. The fact that the P values for both cell size and geometric orientation exceed 0.05, combined with the R^2 value remaining at approximately 35%, indicates a weak predictive relationship. Since this R^2 value is significantly lower than the generally accepted threshold of 85%, it suggests that these parameters do not provide a reliable basis for accurately estimating the absorbed energy of honeycomb cells printed using the FDM method with

PETG. Table 3 shows that the model's accuracy is indicated by the R2 values for force at break (83.56%) and absorbed energy (35.06%).

Table 3. ANOVA for force at break and absorbed energy.

Source	Force at break			Absorbed energy		
	DF	Contribution	P-value	DF	Contribution	P-value
Cell size	2	69.53%	0.037	2	9.38%	0.763
Geometric orientation	2	14.03%	0.291	2	25.68%	0.514
Error	4	16.44%		4	64.94%	
Total	8	100%		8	100%	
R2	83.56%			35.06%		

Figure 9 presents two main effects plots illustrating the impact of cell size and shape orientation on signal-to-noise (S/N) ratios for specific performance metrics. In S/N ratio figures, the highest S/N ratio results in the most optimal settings for operational parameters. In subplot (a), the plot shows S/N ratios for force at break, with distinct trends for each factor. For cell size, the S/N ratio increases as cell size decreases, suggesting that a smaller cell size positively influences the force at break, enhancing the system's robustness to noise. Regarding geometric orientation, a significant variation is observed. An orientation of 15° results in a reduction in the S/N ratio, while orientations of 0° and 30° yield higher ratios, with 30° achieving the highest value. This trend implies that aligning shape orientation to 30° could help optimize force at break. Subplot (b) displays the mean values for absorbed energy across the same factor levels. For cell size, a significant variation is observed again. An orientation of 1.50 mm results in a reduction in the S/N ratio, while orientations of 1.75 and 1.25 mm yield higher ratios, with 1.75 mm achieving the highest value. For geometric orientation, the relationship is again non-linear like cell size. An orientation of 15° leads to notably lower means absorbed energy, whereas an orientation of 30° yields the highest mean value. This observation is consistent with the literature, demonstrating that geometric orientation significantly influences energy absorption capacity [31,32].

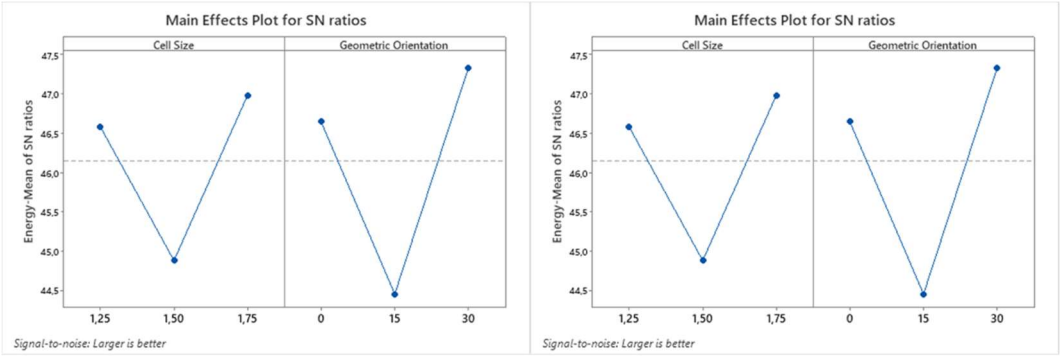

a) b)

Figure 7. S/N ratios of factor levels for (a) force at break and (b) absorbed energy.

4. Conclusions

This study examines the tensile mechanical characteristics of honeycomb structures manufactured with varying cell sizes and geometric orientations, comparing them to specimens fabricated through FDM method using PETG material. The objective of the research was to identify the cell sizes and geometric orientations that yield the highest fracture force and energy absorption. During the production process, configurations with cell sizes of 1.75 mm, 1.5 mm, and 1.25 mm, as well as geometric orientations of 0°, 15°, and 30°, were evaluated. The findings are summarized as follows:

- The highest fracture force (277.03 N) was achieved with a 1.25 mm cell size and a 30° geometric orientation, while the highest energy absorption (335.59 J) was observed in 1.75 mm cell size and a 30° orientation.
- The lowest fracture force (128.43 N) was recorded for the 1.75 mm cell size at a 0° orientation, whereas the lowest energy absorption (151.95 J) was measured in the 1.50 mm cell size at a 15° orientation.
- Cell size accounted for 69.53% of the variation in fracture force, while geometric orientation contributed 25.68% to energy absorption.
- The influence of cell size on both fracture force and energy absorption was greater than geometric orientation.

A systematic evaluation of these parameters enables the advancement and optimization of engineering systems that incorporate honeycomb-structured materials for enhanced performance. The findings from this study hold significant potential for applications in aerospace manufacturing, medical device development, protective equipment, and various other industries where high force resistance, energy absorption, adaptability, and mechanical durability are critical.

This study provides valuable insights; however, it is limited by the specific material, manufacturing parameters, and testing conditions. Future research could expand on these findings by exploring additional variables and employing computational methods to enhance applicability and robustness.

Conflict of Interest Statement

The authors declare that there is no conflict of interest.

References

[1] X. Zhou, L. Ren, Z. Song, and others, "Advances in 3D/4D printing of mechanical metamaterials: From manufacturing to applications," Composites Part B, vol. 254, p. 110585, 2023. doi: 10.1016/j.compositesb.2023.110585

[2] J. Fan et al., "A review of additive manufacturing of metamaterials and developing trends," Materials Today, vol. 50, pp. 303–328, 2021. doi: 10.1016/j.mattod.2021.04.019

[3] Y. Garbatov, S. S. Marchese, G. Epasto, and V. Crupi, "Flexural response of additive-manufactured honeycomb sandwiches for marine structural applications," Ocean Engineering, vol. 302, p. 117732, 2024. doi: 10.1016/j.oceaneng.2024.117732

[4] J. Zhang, G. Lu, and Z. You, "Large deformation and energy absorption of additively manufactured auxetic materials and structures: A review," Compos B Eng, vol. 201, p. 108340, 2020. doi: 10.1016/j.compositesb.2020.108340

[5] C. Qi, F. Jiang, and S. Yang, "Advanced honeycomb designs for mechanical properties: A review," Composites Part B, vol. 227, p. 109393, 2021. https://doi.org/10.1016/j.compositesb.2021.109393. doi: 10.1016/j.compositesb.2021.109393

[6] G. Palomba, G. Epasto, L. Sutherland, and V. Crupi, "Aluminium honeycomb sandwich as a design alternative for lightweight marine structures," Ships and Offshore Structures, vol. 17, pp. 2355–2366, 2022. doi: 10.1080/17445302.2021.1996109

[7] S. L. Omairey, P. D. Dunning, and S. Sriramula, "Development of an ABAQUS plugin tool for periodic RVE homogenisation," Eng Comput (Swansea), vol. 35, pp. 567–577, 2019. doi: 10.1007/s00366-018-0616-4

[8] F. Pehlivan, F. H. Öztürk, S. Demir, and A. Temiz, "Optimization of functionally graded solid-network TPMS meta-biomaterials," J Mech Behav Biomed Mater, vol. 157, p. 106609, 2024. doi: 10.1016/j.jmbbm.2024.106609

[9] G. Sun, X. Huo, H. Wang, and others, "On the structural parameters of honeycomb-core sandwich panels against low-velocity impact," Composites Part B, vol. 216, p. 108881, 2021. doi: 10.1016/j.compositesb.2021.108881

[10] Z. Huang, X. Zhang, and C. Yang, "Experimental and numerical studies on the bending collapse of multi-cell Aluminum/CFRP hybrid tubes," *Composites Part B*, vol. 181, p. 107527, 2020. doi: 10.1016/j.compositesb.2019.107527

[11] A. Singh, B. Koohbor, and G. Youssef, "Full-field characterizations of additively manufactured composite cellular structures," *Composites Part B*, vol. 272, p. 111208, 2024. doi: 10.1016/j.compositesb.2024.111208

[12] X. Zheng, T. Chen, X. Jiang, and others, "Deep-learning-based inverse design of three-dimensional architected cellular materials with the target porosity and stiffness using voxelized Voronoi lattices," *Sci Technol Adv Mater*, vol. 24, p. 2157682, 2023. doi: 10.1080/14686996.2022.2157682

[13] P. Nampally, A. T. Karttunen, and J. N. Reddy, "Nonlinear finite element analysis of lattice core sandwich plates," *Int J NonLinear Mech*, vol. 121, p. 103423, 2020. doi: 10.1016/j.ijnonlinmec.2020.103423

[14] H. Yang, Z. Liu, Y. Xia, and others, "Mechanical properties of hierarchical lattice via strain gradient homogenization approach," *Composites Part B*, vol. 271, p. 111153, 2024. doi: 10.1016/j.compositesb.2023.111153

[15] L. Mizzi, D. Attard, R. Gatt, and others, "Implementation of periodic boundary conditions for loading of mechanical metamaterials using finite element analysis," *Eng Comput (Swansea)*, vol. 37, pp. 1765–1779, 2021. doi: 10.1007/s00366-019-00910-1

[16] Z. Zhao, C. Liu, X. Xu, L. Sun, J. Wang, Y.Li, "An FFT-based method for estimating the in-plane elastic properties of honeycomb considering geometric imperfections at large elastic deformation," *Thin-Walled Structures*, vol. 185, p. 110570, 2023. doi: 10.1016/j.tws.2023.110570

[17] A. F. Yilmaz and M. Konal, "Enhanced Container Ship Hatch Cover using Topology Optimization Method for Lightweight Design and Optimal Costs," *Journal of Offshore Mechanics and Arctic Engineering*, pp. 1–16, 2025. doi: 10.1115/1.4067799

[18] T. Wu, M. Li, X. Zhu, and X. Lu, "Research on non-pneumatic tires with gradient anti-tetrachiral structures," *Mechanics of Advanced Materials and Structures*, vol. 28, pp. 2351–2359, 2021. doi: 10.1080/15376494.2020.1734888

[19] S. Liu, F. Zhang, B. Chao, and others, "Based on the preparation of dual-absorber agents using Ni and Ni/rGO for the fabrication of a dual honeycomb nested structure for wideband microwave absorption," *Composites Part B*, vol. 284, p. 111735, 2024. doi: 10.1016/j.compositesb.2024.111735

[20] X. Zhang, L. Zhang, and P. Zhang, "Equivalent constitutive equations of honeycomb material using micro-polar theory to model thermo-mechanical interaction," *Composites Part B*, vol. 43, pp. 3081–3087, 2012. doi: 10.1016/j.compositesb.2012.04.056

[21] Y. Le, N. S. Ha, and N. S. Goo, "Advanced sandwich structures for thermal protection systems in hypersonic vehicles: A review," *Composites Part B*, vol. 226, p. 109301, 2021. doi: 10.1016/j.compositesb.2021.109301

[22] C. Peng and P. Tran, "Bioinspired functionally graded gyroid sandwich panel subjected to impulsive loadings," *Composites Part B*, vol. 188, p. 107773, 2020. doi: 10.1016/j.compositesb.2020.107773

[23] X. Xing, S. Yang, S. Lu, and others, "Energy absorption and optimization of bi-directional corrugated honeycomb aluminum," *Composites Part B*, vol. 219, p. 108914, 2021. doi: 10.1016/j.compositesb.2021.108914

[24] F. Pehlivan, "Optimizing 3D-Printed Auxetic Structures for Tensile Performance: Taguchi Method Application on Cell Size and Shape Orientation," *Manufacturing Technologies and Applications*, vol. 5, no. 3, pp. 284–294, 2024. doi: 10.52795/mateca.1576416

[25] S. Demir, A. Temiz, and F. Pehlivan, "The investigation of printing parameters effect on tensile characteristics for triply periodic minimal surface designs by Taguchi," *Polym Eng Sci*, vol. 64, no. 3, pp. 1209–1221, 2024. doi: 10.1002/pen.26608

[26] N. Ben Ali, M. Khlif, D. Hammami, and C. Bradai, "Experimental optimization of process parameters on mechanical properties and the layers adhesion of 3D printed parts," *J Appl Polym Sci*, vol. 139, no. 9, p. 51706, 2022. doi: 10.1002/app.51706

[27] F. H. Öztürk, "Optimization of adherend thickness and overlap length on failure load of bonded 3D printed PETG parts using response surface method," *Rapid Prototyp J*, vol. 30, no. 8, pp. 1579–1591, 2024. doi: 10.1108/RPJ-02-2024-0090

[28] A. F. Yilmaz, "Assessment of Combinability of S235JR-S460MC Structural Steels on Fatigue Performance," *Transactions of the Indian Institute of Metals*, vol. 77, no. 2, pp. 323–331, Feb. 2024. doi: 10.1007/s12666-023-03113-x

[29] P. Wang, Y. Bian, F. Yang, H. Fan, and B. Zheng, "Mechanical properties and energy absorption of FCC lattice structures with different orientation angles," *Acta Mech*, vol. 231, pp. 3129–3144, 2020. doi: 10.1007/s00707-020-02710-x

[30] A. Temiz, "The Effects of Process Parameters on Tensile Characteristics and Printing Time for Masked Stereolithography Components, Analyzed Using the Response Surface Method," *J. of Materi Eng and Perform.*, vol. 33, pp. 9356–9365, 2024. doi: 10.1007/s11665-023-08617-7

[31] M. Günay, S. Gündüz, H. Yılmaz, N. Yaşar, and R. Kaçar, "PLA Esaslı Numunelerde Çekme Dayanımı İçin 3D Baskı İşlem Parametrelerinin Optimizasyonu," *Politeknik Dergisi*, vol. 23, no. 1, pp. 73–79, Mar. 2020. doi: 10.2339/politeknik.422795

[32] M. Xu, Z. Xu, Z. Zhang, H. Lei, Y. Bai, and D. Fang, "Mechanical properties and energy absorption capability of AuxHex structure under in-plane compression: Theoretical and experimental studies," *Int J Mech Sci*, vol. 159, pp. 43–57, 2019. doi: 10.1016/j.ijmecsci.2019.05.044